IEEE Access
Multidisciplinary | Rapid Review | Open Access Journal

Received 6 July 2022, accepted 8 August 2022, date of publication 22 August 2022, date of current version 31 August 2022.

Digital Object Identifier 10.1109/ACCESS.2022.3200748

APPLIED RESEARCH

Optical Detection of Partial Discharges Under Fast Rising Square Voltages in Dielectric Liquids

SOMYA ANAND[1,2], ERIC VAGNON[1,2], (Member, IEEE), MARTIN GUILLET[1], AND CYRIL BUTTAY[2], (Senior Member, IEEE)

[1]Power Electronics and Converter, SuperGrid Institute, 69628 Villeurbanne, France
[2]Ampère UMR5005, CNRS, Ecole Centrale de Lyon, INSA Lyon, Université Lyon 1, 69130 Ecully, France

Corresponding author: Eric Vagnon (eric.vagnon@ec-lyon.fr)

ABSTRACT Partial discharge (PD) measurement of an insulation system is widely used as a diagnostic tool for the quality control of high voltage apparatuses. In ac, the conventional method of PD detection is well established. However, under square voltages such as those generated across power electronic converters, the conventional method cannot discriminate between PDs and switching transients. In this context, this paper demonstrates PD detection under fast-rising square voltages by deploying a photomultiplier tube. For this, an experimental set-up generating unipolar square voltage (USV) waveforms is developed, generating a dV/dt in the range of 10-100 kV/μs. The device under test (DUT) comprises of needle-barrier plane configuration immersed in dielectric liquids. Barriers differing in permittivity and thicknesses are chosen to test with two types of dielectric liquids, to assess varying conditions. The results thus obtained show a lower partial discharge inception voltage (PDIV) in USV than in bipolar ac for the same DUT specimen. The phase-resolved (PR) PD patterns exhibit a higher PD occurrence during rising and falling front of the USV waveform. Experimental results demonstrate the relevance of the PMT as a PD detector for square voltage waveforms exhibiting high dV/dt in dielectric liquids.

INDEX TERMS Partial discharge, square voltages, high dV/dt, ac, optical method, photomultiplier tube, high divergent field, dielectric liquids.

I. INTRODUCTION

In the drive to increase the flow of power density, minimize the switching losses and build more compact equipment, there has been a significant evolution in power electronic devices in terms of voltage level, switching speed, and repetition rate. The recent introduction of silicon carbide (SiC) switches has even raised the standards by offering breakdown voltages as high as 15 kV, switching speeds of about 100 kV/μs, and operating frequencies higher than 100 kHz [2], [3]. Such characteristics increase the stresses on the insulation systems as numerous studies have shown that the fast repetitive square voltages can accelerate the degradation of the insulation system of the equipment [3], [4], [5], [6]

For high voltage (HV) applications, Partial Discharge (PD) measurement can be used as a tool to assess the insulation quality, for instance as an aging indicator or as a qualification test before commissioning. In case of ac, the high-frequency PD signals are segregated from low-frequency (50 or 60 Hz) ac waveforms by implementing a bandpass filter as specified in IEC 60270 [7]. However, under square voltages, the frequency spectra of switching transients generated by fast switches overlaps with the PD signals. The separation of the PD events from switching transients is then difficult using the standard electrical method of IEC 60270.

This situation makes it important to look for other methods of PD measurement under fast repetitive square waveforms [8], [9]. For PD measurement under repetitive voltage impulses, the IEC 61934 standard [10] recommends non-conventional techniques such as antenna, high-frequency current transformer (HFCT), and coupling capacitor. But the studies conducted with the HFCT in [11] and [12] and with an antenna in [13] have shown that the EMIs generated by the switching transients (with a voltage rise time (t_r) < 1 μs) hinder the PD detection. With the coupling

The associate editor coordinating the review of this manuscript and approving it for publication was Sudhakar Babu Thanikanti.

capacitor (typically in hundreds of pF), when put in parallel to tens of pF (usual value of a device under test (DUT) in a laboratory), would slow down the voltage transients substantially compared with those observed in real conditions. Some other studies like [11] and [14] have shown the implementation of optical detectors such as photomultiplier tubes for PD measurement in square voltages which detects the photons emitted during the discharge process and offers high immunity against the EMIs generated from high speed switching. Like optical detectors, the acoustic sensors are also immune to EMIs [1], [15] and have attracted the attention of many research groups for PD localization in large equipment such as gas insulated substation (GIS) and transformers. But, with these techniques, the methodology of PD detection and experimental results are quite limited under square voltages. Some other studies have proposed the stochastic detection of PDs under square voltage waveform by deploying techniques such as a PD coupler circuit [8], balanced bridge circuit [16] and standard deviation technique [17]; but their implementation is extremely sensitive to the components of the test systems and to their arrangement to minimize the electromagnetic interferences (EMI) from high-speed switching.

Most of aforementioned PD studies are done with solid insulators to address winding insulation. Investigations in liquid or solid/liquid systems are quite limited; [18] addresses oil/pressboard insulation system under square voltage, but with a $t_r \approx 0.1$ ms; [19] presents PD investigation for rise times in the range of 300 to 1000 ns for impregnated kraft paper in plane-plane configuration, with a dV/dt of less than 20 kV/μs at PDIV; while [14] has discussed the PD detection in liquid embedded PCB model.

Liquid and solid/liquid insulation systems are the most relevant solution for some HV applications, due to their superior thermal and dielectric behavior [4], [5], [6]. Elements such as transformers in medium voltage dc systems (MVDC) can implement solid liquid insulation systems and experience very fast switching transients. Therefore, there is a need for test systems allowing to expose insulation systems to realistic waveforms and detect the possible occurrence of PDs.

In this paper, we demonstrate the optical detection of PDs under high dV/dt (10-100 kV/μs and $t_r < 300$ ns) in dielectric liquids, taking advantage of the optical transparency of insulating liquids. The test system comprising a unipolar square voltage (USV) generator, a Photo-Multiplier Tube (PMT) is presented in section II. The custom device under test (DUT), designed to maximize PD generation is introduced in section III, tested in both ac and USV. As dielectric liquids, mineral oil and synthetic ester are chosen based on their applications in HV apparatuses [18], [20]. Barriers with varying permittivity and thickness, finding applications in HV apparatuses are chosen. The partial discharge inception voltage (PDIV), phase resolved (PR) PD pattern, obtained under both waveforms are compared to evaluate the PD phenomenon between the two waveforms.

II. EXPERIMENTAL SET-UP

Figure 1 demonstrates the schematics of test benches generating ac and square voltages inside the same faraday cage. For PD tests in ac, the test circuit complies with the IEC 60270 standard with a maximum voltage rating of 25 kVrms. The ac voltage is remotely controlled using an in-house developed Arduino board, which controls an amplifier kept outside the cage. This amplifier sends the low voltage ac signal to a transformer (24 V/230 V) to regulate the output voltage from PD free transformer. The PD measurement is realized by a commercially available detector (comprising of coupling capacitor C_k of 1 nF, measuring impedance Z_{mi}, and commercially available PD measurement system (Omicron MPD 600)) as well as with the PMT (Hamamatsu R943-02). Two PD measurement units are coupled together for synchronized PD detection as described in our previous work [21]. For the ac tests, the HV connections PR is made inside the cage, while the operator connects to the Arduino board via a USB cable (LN).

The unipolar square voltage is generated by an HV switch (Behlke HTS 1401-10-LC2, maximum repetition rate 500 Hz). The circuit includes a 30 kV/5 kW dc generator, a 4 μF/50 kV capacitor bank (C), and three HV resistors (R1, R2, R3), with values provided in Table 1,

TABLE 1. Resistor values used in square voltage generation.

R1	R2	R3
8.5 kΩ	2 MΩ	5 kΩ

The resistor R1 limits the current from the dc generator and thus sets the time constant for charging C. The chosen value of R2 ensures a limited current when the switch closes, and makes sure the discharging of the DUT when the switch opens, setting the falling time of the USV. R3 is used to keep the current below the HV switch rating in case the DUT fails.

For PD detection in USV, the measurement system is built around the PMT. Its spectral response ranges from 160 to 930 nm, which covers the wavelength of light emitted from corona discharges in air (about 400 nm) and PDs in transformer oil (usually between 350 and 700 nm) [22], [23]. To block the ambient light, the DUT is placed inside a dark metallic enclosure, in the line of sight of the PMT as shown in Figure 1. A dc source connected to the PMT controls its gain: a larger negative bias (up to −2.2 kV) increases the gain (or luminous sensitivity) of the PMT, at the cost of larger dark current (background noise). Therefore, the dc bias must be adjusted to ensure high sensitivity, while maintaining dark current at a low enough level to allow detection of faint light signals such as those emitted by PDs [23]. This is discussed in section IV. The output signal of the PMT is acquired by either using a commercially available PD measurement unit, with a bandwidth of 20 MHz, or with the

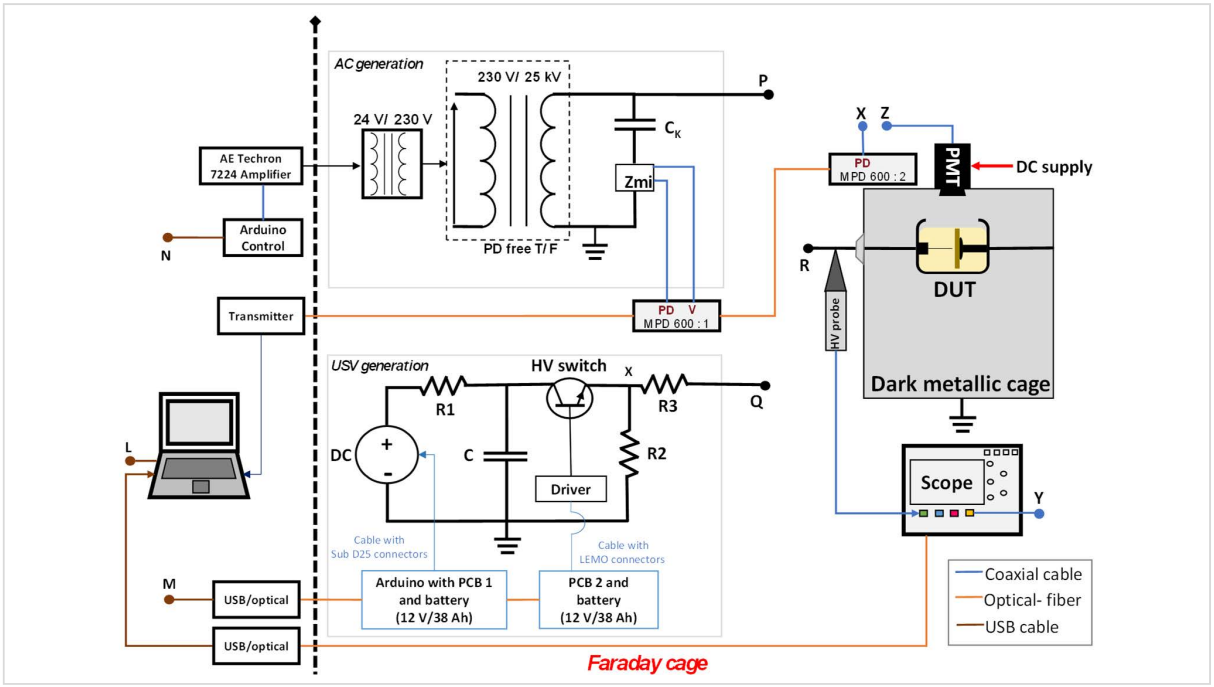

FIGURE 1. Schematics of the test bench showing the AC and USV generation in the faraday cage with the measurement system and the remote control unit.

scope (Tektronix MDO34, bandwidth 200 MHz), as shown in Figure 1.

As the optical detection does not provide a direct measurement of the PD charge, PDs measured by this method are reported here in arbitrary units (a.u.). The control signal of the HV switch (from PCB2) is also fed to the PD measurement system to provide synchronized PD detection in USV waveform.

In addition to the PMT signal, the voltage across the DUT (V_{DUT}) is measured with an HV probe (Tektronix P6015A, bandwidth 75 MHz) using the oscilloscope, as shown in Figure 1.

Finally, the test bench is remotely controlled using fiber optics to ensure user safety and prevent the transmission of the EMI. A custom circuit (located inside the Faraday cage and remotely driven using fiber optics, PCB 1 and PCB 2) controls the switching frequency and duty cycle of the HV switch, as well as the voltage level of the dc source. As the fast transient voltages of the USV are prone to generate strong level of EMI, some mitigation measures have been implemented in the test bench. In addition to the fiber optics communication wherever possible, these include the use of a battery (12 V) for powering the control circuit, the HV switch accessories (cooling pump, heat-exchanger, gate driver); metallic shielding of the HV connection nodes; short-length shielded coaxial cables with ferrite cores to limit common mode currents. For PD tests in USV the point Q is connected to R inside the cage and L to M for remote control.

III. DEVICE UNDER TEST (DUT)

For the PD tests, a needle-barrier-plane configuration immersed in the dielectric medium is chosen, as shown in Figure 2. The geometry allows the generation of a high electric field at the needle tip (radius $= 1\ \mu$m), ensuring strong PD generation at a voltage level compatible with our test system (30 kV max, limited by the dc supply, and 25 kV in ac). The solid barrier limits the risk of a breakdown during the tests, as recommended in the datasheet of the HV switch [25] to prevent any damage. Table 2 details the parameter and geometry of the DUT used for the PD tests.

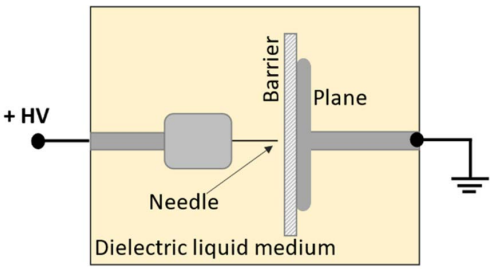

FIGURE 2. The device under test with needle-barrier-plane immersed in a dielectric liquid.

A. DUT PREPARATION

Two commercially-available dielectric liquids are used here: a mineral oil (Nytro 4000X) and a synthetic ester (Midel 7131). Prior to the PD tests, the dielectric liquids are filtered with a sintered glass filter (porosity grade 4) with pore

TABLE 2. Parameters of the DUT Specimen.

Parameters	Type/dimension
Electrode configuration	Needle- barrier-plane
Needle tip radius	1 µm
Barrier ($l \times b$)	40 mm × 40 mm
Plane electrode diameter	20 mm
Medium	Dielectric liquid
Gap (needle tip to the barrier)	0.7 mm

diameter ranging between 10-16 μm, and a vacuum pump which creates a pressure less than 1 mbar. Following the filtration, the liquids are monitored by inspecting their breakdown voltage (BDV) and water content (WC) values. The BDV tests are performed in compliance with IEC 60156:1995 standard procedure in a commercial system (BAUR DTA 100 C), while water content is measured using coulometric Karl Fischer (KF) titration [26]. The mean of thirty BDV tests and two WC measurements are provided in Table 3, along with their respective datasheet values, provided in [27] and [28]. As can be seen in Table 3, the measured values are compliant with their corresponding datasheet values.

TABLE 3. Properties of dielectric liquids used for pd tests [27], [28].

Properties	Mineral oil (Nytro 4000X)		Synthetic ester (Midel 7131)	
	In datasheet	Measured	In datasheet	Measured
Breakdown voltage (kV)	> 70	> 75 (mean of 30 BDV tests)	> 75	> 80 (mean of 30 BDV tests)
Water content (ppm)	< 20	< 12 (mean of 2 WC tests)	< 200	< 130 (mean of 2 WC tests)

Three barrier materials are used during the PD test campaign: polyvinyl chloride (PVC), glass-reinforced epoxy (FR4) and aluminum nitride (AlN). These materials offer a range of permittivity values (see Table 4) and for each material, two barrier thicknesses are investigated, to ensure a variety of test cases. The barrier samples are wider (40 mm × 40 mm) than the grounding electrode (20 mm diameter) to prevent flashovers during the PD tests.

Before test, the barrier samples are cleaned in isopropanol, dried for around 4 hours at 45 °C. Those which are not used immediately are stored in airtight boxes.

In the reminding of the article, a ''DUT specimen'' designates a set comprising of dielectric liquid, a needle and a barrier sample. Treated dielectric liquid, new needles and new barriers are used for each DUT specimen.

IV. PRELIMINARY INVESTIGATION

This section summarizes the characteristics of the USV test bench for achievable rise time and repetition rate of the output voltage. Further, some preliminary tests are conducted using the PMT to realize the PD acquisition.

TABLE 4. Solid barriers used for pdiv tests.

Barrier samples	Type	Thickness (mm)	Samples tested in mineral oil (ε_r=2.2)	Samples tested in ester (ε_r=3.2)
PVC (ε_r=2.24)	Polymer based	1	5	5
		2	5	5
FR4 (ε_r=4.2)	Composite (fiberglass with epoxy)	0.7	5	5
		1.3	5	5
AlN (ε_r=8.5)	Inorganic	0.63	3	3
		1	3	3

Note: references for permittivity [18], [29], [30]

A. OUTPUT VOLTAGE WAVEFORMS

For these tests, a DUT specimen (Figure 2) is used as load. The voltage generated across resistor R2 (V_{R2} at node 'X' in Figure 1) and V_{DUT}(at node 'R') are measured at the same supply voltage level. The rising times (10 % to 90 % of the final value) of V_{R2} and V_{DUT} are found to be around 30 ns and 256 ns respectively, as shown in Figure 3. This corresponds to a slew rate of around 78 kV/μs at 20 kV across the DUT. Furthermore, the resistance R3 being 5 kΩ, the capacitance of DUT can be estimated to be 23 pF.

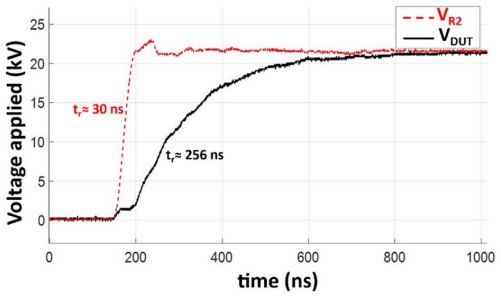

FIGURE 3. Rising times of the voltage across the resistance R2 (V_{R2}) and the DUT (V_{DUT}) at 20 kV.

Figure 4 shows V_{DUT} at a switching frequency of 460 Hz at 20 kV. The longer falling time of about 350 μs is due to the large value of resistance R2 in the circuit, which also limits any further increase in switching frequency. At the end of one voltage cycle, the DUT can be considered as discharged with less than 3 % voltage remaining.

B. MEASUREMENT SIGNALS

Next, the behavior of the PMT signals is studied. In the first step, the PMT is coupled to the oscilloscope using a coaxial cable. The needle of the DUT is removed (to prevent PDs to occur) and the power supply of the PMT is turned off (to prevent the detection of any light signal). During this investigation, the PMT signal is found to be disturbed by the EMI generated by the fast switching action of the HV switch (see Figure 5). This disturbance spans almost over 300 ns

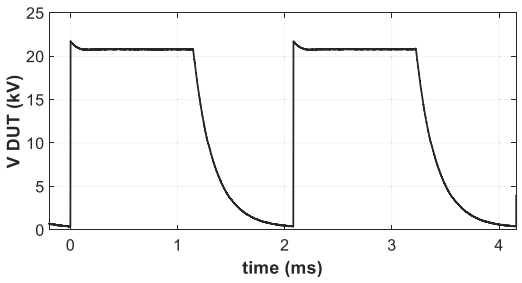

FIGURE 4. V_{DUT} with switching frequency of 460 Hz and 50 % duty cycle.

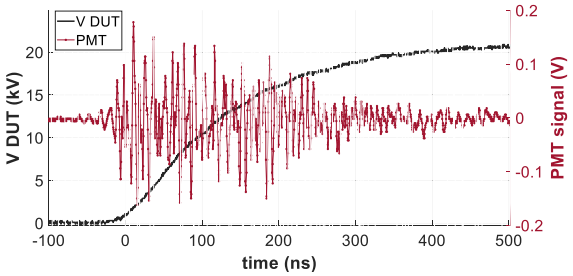

FIGURE 5. Disturbance observed on PMT signal at 20 kV due to EMI generated from high-speed switching (DC supply of PMT turned off).

on the PMT signal, almost the same as the rise time across the V_{DUT}, and can be observed despite the EMI mitigation measures described above.

The disturbance on the PMT signal is also tested by coupling the PMT with the PD measurement system. The measurement system integrates the acquired signals and display them as phase-resolved patterns. Figure 6 presents a pattern without any needle in the DUT at 20 kV. As the acquisition is done using the PMT, the chart scale presented in Figure 6 is reported in pa.u. scale and not in pC. In the pattern, a background noise floor of less than 0.2 pa.u. is present, which is same as reported in our previous work [21]. Apart from this, a small peak of around 0.4 pa.u. is observed during commutation, even with the DC supply of the PMT turned-off. Compared with the oscilloscope measurements (Fig. 5), the PD measurement system performs a frequency-domain integration on the disturbances carried by the coaxial cable, which brings them down to a level comparable to the background noise floor, which is considered acceptable here.

C. DETERMINATION OF PD OCCURRENCE

For this investigation a DUT specimen with a needle, FR4 as a barrier and ester as dielectric liquid is used. In the first step, the acquisitions are made using the oscilloscope. The DC supply of the PMT is kept at −2 kV and the voltage across the DUT is slowly raised from 0 V. At 20 kV, the negative peaks (marked as PD1 to PD6 in green) are observed just after the rising front and along the DC plateau region of the V_{DUT}, as shown in Figure 7.

To ensure these negative peaks correspond to PD events, two other conditions are also tested: turning off the DC supply of the PMT with DUT untouched; and removing the needle

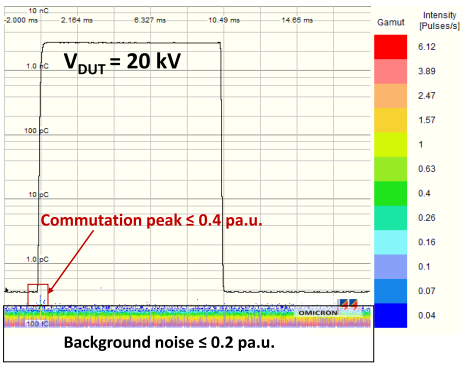

FIGURE 6. Commutation peak observed with the PMT signal at 20 kV when coupled with PD measurement system besides the background noise (DC supply of PMT turned off); the square voltage is acquired by synchronizing the control signal of the driver.

from the DUT with the DC supply of the PMT at −2 kV. The V_{DUT} is kept at 20 kV for both cases. The waveforms thus acquired for these conditions are also plotted in Figure 7. As can be seen, the negative peaks are not detected for these two conditions. The commutation noise can be seen overlapping with each other for all three cases i.e., DUT with needle with PMT at −2 kV, DUT without needle with PMT at −2 kV, and PMT switched off for DUT with needle. This demonstrates that the negative peak signals from the PMT correspond to the detection of photons produced by the PDs.

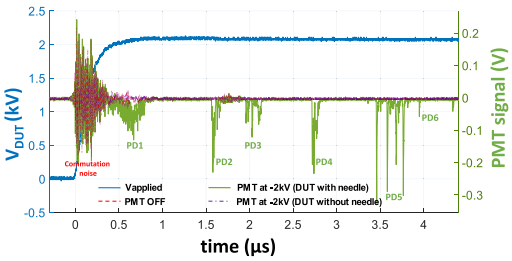

FIGURE 7. Acquisition of PDs (PD1 to PD6 in green) at 20 kV; verification of the PD occurrence by turning off the DC supply of the PMT and removing the needle from the DUT by stressing the DUT by same voltage, when no PDs occurred.

The tests are also carried out by varying the DC supply of the PMT to find the optimized value in the experimental conditions. Decreasing the absolute value of the (negative) PMT supply, reduces the sensitivity of the PMT. On the contrary, increasing the PMT supply increases sensitivity, at the cost of higher background noise.

Figure 8 shows the PRPD pattern recorded after 30 s with the DC supply of PMT at −2 kV and V_{DUT} at 20 kV. The acquired charges can be classified in two groups, charges below 5 pa.u. and charges above 5 pa.u. The band of charges below 5 pa.u. is mainly due to the dark current (background noise) generated by the PMT at −2 kV, while those above it are PD events (as marked in Figure 8). This is verified by removing the needle from the DUT, resulting in the disappearance of charges of more than 5pa.u. as shown in Figure 9.

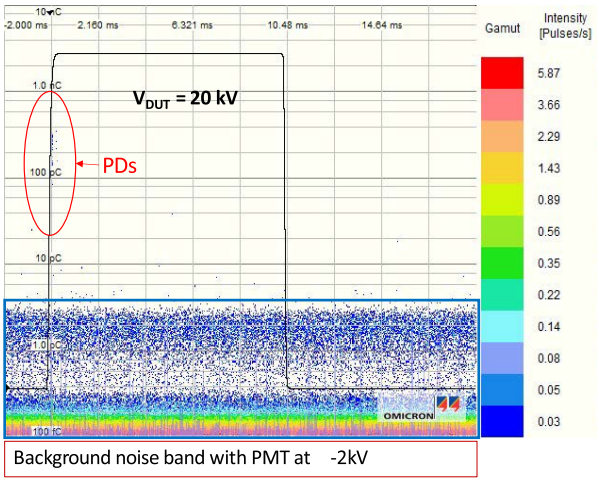

FIGURE 8. PDs (encircled in red) and dark current (encircled in blue) with the PMT DC supply at −2 kV with V_{DUT} at 20 kV; the DUT is equipped with a needle.

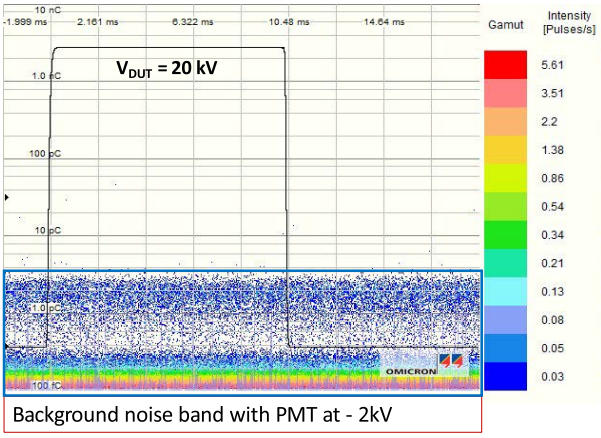

FIGURE 9. Dark current (encircled in blue) with the PMT DC supply at −2 kV with V_{DUT} at 20 kV; the DUT is without needle.

The DC supply of PMT is then reduced to −1.3 kV, keeping all other parameters identical (this value of −1.3 kV has been used during previous test campaigns [21]). Similar PDs are found to be detected with this reduced bias as with the −2 kV dc supply, as shown in Figure 10. The PD occurrence is reconfirmed by following the same steps as before, i.e. turning off the PMT supply and removing the needle. The noise peak due to commutation and background noise floor in Figure 10 are almost same as presented earlier in Figure 6 (with the PMT dc supply turned off).

As a result of these tests, −1.3 kV is found to be sufficient to detect PDs in dielectric liquid for our experimental conditions (with a distance between the PMT lens and the DUT of approximately 25 cm). This is also compliant with the PMT specifications from Hamamatsu [24], which recommends to operate it between −700 V and −1.4 kV for best signal-to-noise ratio.

In summary, it is found that the detection of PD peaks with the PMT and an oscilloscope is difficult because of the large commutation noise and the single-event acquisition.

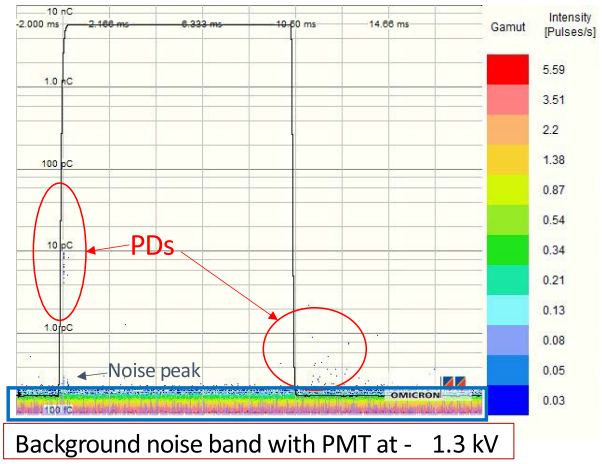

FIGURE 10. PD acquisition with DC supply of PMT at −1.3 kV for VDUT at 20 kV; the DUT is equipped with a needle.

This requires increasing the dc bias of the PMT to −2 kV to increase the gain of the PMT. On the contrary, the acquisition of the PDs is found to be easier with the PD measurement system (low switching noise due to the integration system, superimposition of many acquisitions), allowing the dc bias to be kept at the recommended level of −1.3 kV. Therefore, for further investigations, the PMT coupled with a PD measurement system is chosen. However, due to an impedance mismatch between the PD measurement unit and the HV probe, it is necessary to use the oscilloscope to monitor V_{DUT}: the square waves (black lines) visible in the PRPD patterns of, e.g. Figs. 8 to 10 correspond to the logic signal sent to the switch, not to actual measurements of V_{DUT}, and are used for synchronization only (the actual V_{DUT} waveform is visible in Fig. 4).

V. METHODOLOGY OF PD TESTS IN AC AND USV

This section presents the strategy adopted for PD comparison between ac 50 Hz and USV 50 Hz. The commutation peak found during preliminary tests (Figure 6), is about 0.4 pa.u. at 20 kV, so a threshold value of 0.5 pa.u. is chosen for PDIV detection under both ac and USV. To compare the PDIV results between both kinds of waveforms, voltages obtained in ac 50 Hz are reported as peak-peak values ($=2\sqrt{2} \times V_{rms}$). For USV, the amplitude values are reported (zero to peak).

The electrical and optical measurements are used simultaneously in ac, for validation and calibration of the optically acquired PDs with the electrical detection method [21]. Before starting the tests, the voltage and charge calibration are done for the electrical method as recommended in IEC 60270 standard. In USV, only the optical method is used.

For the PD measurement in ac and USV waveform, the voltage profile shown in Figure 11 is adopted.

To allow comparisons between different specimens and minimize marginal effects, it is necessary to make a pre-conditioning to ensure the same initial electrical state of the specimens. Therefore, in the first step the voltage is increased by ramp until the first PD occurrence and

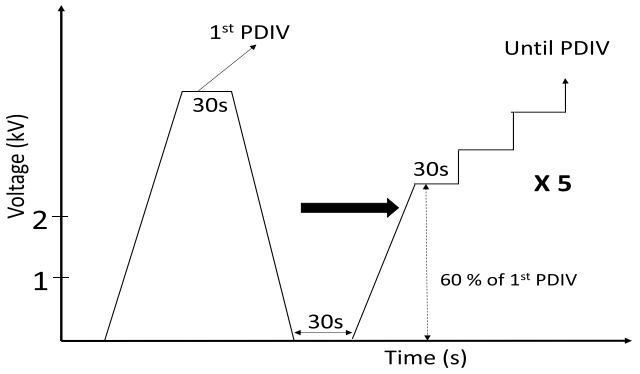

FIGURE 11. Voltage profile for PDIV comparison between square and ac voltages.

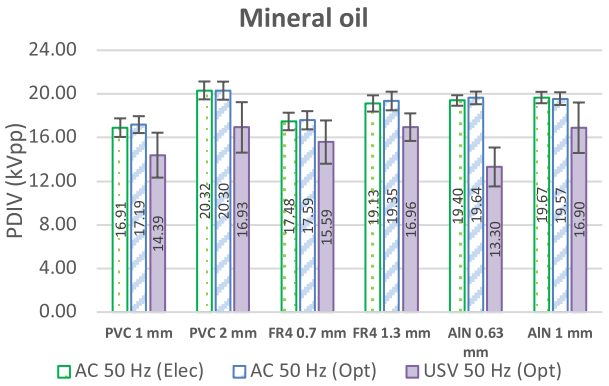

FIGURE 12. Average PDIV of different barriers tested in mineral oil; using electrical and optical detection in ac and optical detection only in USV; the threshold in electrical detection is 2 pC while it is 0.5 pa.u. for optical detections.

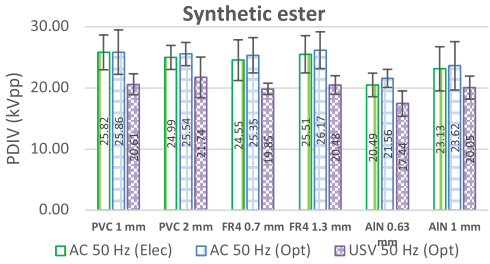

FIGURE 13. Average PDIV of different barriers tested in synthetic ester; using electrical and optical detection in ac and optical detection only in USV; the threshold in electrical detection is 10 pC while it is 0.5 pa.u. for optical detections.

maintained for 30s before stopping. This step also gives the range of the 60% of PDIV. After a rest time of 30 s at 0 V, the voltage is again increased to 60 % of the PDIV found in the previous step. Then the voltage is increased in 1 kV steps with a waiting time of 30 seconds until PDIV is achieved again. This step is repeated five times. An interval of 30 seconds at zero voltage is kept between two successive voltage applications to prevent accumulation of charges in the DUT specimen. Unlike a continuous ramp voltage profile, the stepped voltage profile allows the acquisition of PD parameters over 30 seconds at PDIV, which can be used for further analysis. All tests are carried out according to IEC60270 criteria, which implies that the PDIV is the lowest voltage at which PD(s) begin to occur. Three or five DUT specimens are used for each configuration (see Table 4); each DUT specimen undergoes ten PD measurements, five each under ac and five under USV waveform (with half of the specimens undergoing ac tests before USV, and another half in USV before ac to ensure reproducibility of tests).

VI. PARTIAL DISCHARGE RESULTS

A. VALIDATION OF THE PMT IN AC 50 Hz

Figures 12 and 13 show the average PDIV values measured in ac (optical and electrical method) and USV (optical method), for all barrier/liquid configurations. The error bars correspond to the standard deviation (SD). Thanks to the synchronized PD detection in ac, a correlation is established between optically-, and electrically-acquired PDs, using the strategy discussed in [21] and [31]. The optically-acquired PDs of 0.5 pa.u. magnitude are hence found to correspond to 2 pC in mineral oil, and 10 pC in ester. For the abovementioned values, similar PDIVs are obtained from electrical (green bars) and optical (blue bars) detection methods. This is found to be true for all barriers tested in both dielectric liquids, for the tested experimental conditions (dc supply of the PMT set at −1.3 kV, 250 mm gap between PMT lens and DUT).

B. PD COMPARISON BETWEEN AC AND USV

The optical method clearly shows that average PDIVs acquired under USV (purple bars) are lower than in ac (blue bars) for all combinations of liquid/solid tested (Figure 12 and 13). To assess if the difference in average value of PDIV is significant between ac and USV, t-test method is applied (see Appendix for explanation on t-test). For t-test, 0.05 is taken as the p-value, as evidence against the null hypothesis. Apart from the p-value, the SD, 95 % confidence interval (CI) with upper bound (UB) and lower bound (LB) are also determined. The values are presented in Table 5. As can be observed from these tables, for each barrier tested under ac and USV waveforms, the p-value is less than 0.05. This is true in both dielectric liquids, which indicates a significant difference in average PDIV values between ac and USV for test cases.

Using the expression given in (1), the percentage decrease in average PDIV of the USV is calculated in the next step. The values thus obtained are presented in Table 6.

From Table 6, the highest reduction in PDIV in USV can be noticed for 0.63 mm AlN in mineral oil (32 % reduction). In ester, the highest reduction is observed for composite FR4 barriers (22%) but in mineral oil, it is larger for FR4 barriers (11-12%).

$$\%\ decrease = \frac{(Average\_PDIV_{AC} - Average\_PDIV_{USV}) \times 100\%}{Average\_PDIV_{AC}} \quad (1)$$

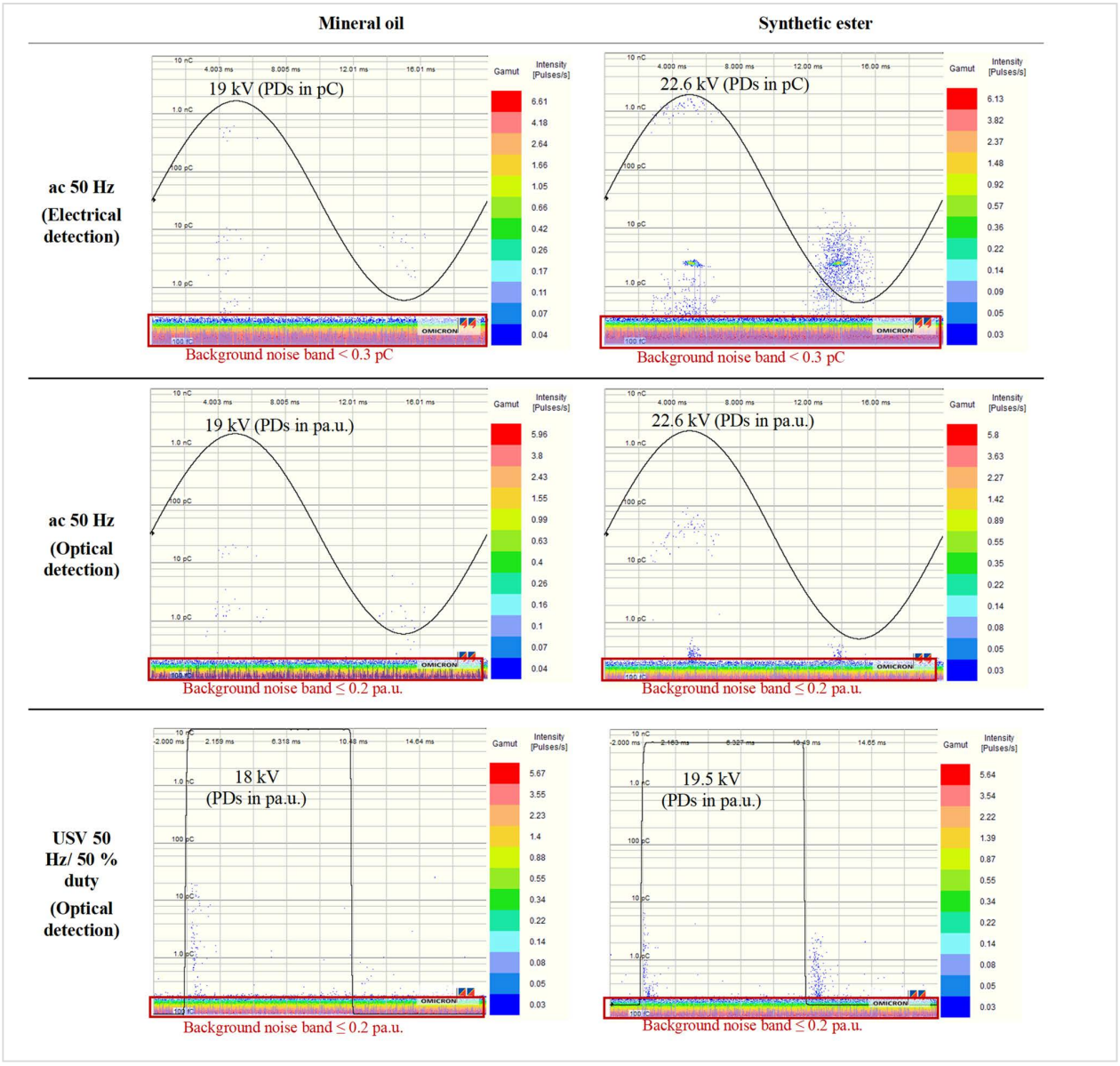

FIGURE 14. PRPD patterns acquired in ac (from electrical and optical detection) and USV (only using optical detection) at PDIV in mineral oil and synthetic ester for 0.7 mm thick FR4 barrier. Note: the PRPD patterns presented here are from same DUT specimen in each dielectric liquid. The square voltage represents the control signal fed to the driver of HV switch.

C. PRPD COMPARISON BETWEEN AC AND USV

Figure 14 presents the PRPD patterns captured after 30 seconds at PDIV for 0.7 mm-thick FR4 barriers in both mineral oil and ester. The PRPDs are acquired from the same DUT specimen for each liquid (using both electrical and optical detection in ac, and optical detection only in USV). The noise floor is lower than 0.3 pC for electrical detection, and lower than 0.2 pa.u. for optical detection.

In ac, the PDs can be seen appearing around the voltage crests (phase angles of 90° and 180°) in both the positive and the negative half-cycles of the sinusoidal voltage, from both detection techniques. As compared to the electrical method, the optical method shows a lower sensitivity in detection of same set of PD clusters. The lower sensitivity can be associated with the attenuation of light in the dielectric liquid medium [32].

Furthermore, the higher occurrence of PD in ester than in mineral oil can be observed with both detection methods (although it is more obvious with the electrical detection method). The higher voltage at PDIV and higher water content of the ester (see Table 3) favors PD initiation compared to the mineral oil, leading to higher occurrence of PD events in ester [33]. Under USV, the acquired PRPD patterns show PDs mainly around the rising and falling parts of the square signal.

TABLE 5. Estimation of difference in the average value of pdiv between ac and usv for mineral oil and synthetic ester using T-test.

Mineral oil												
Barriers	PVC 1 mm		PVC 2 mm		FR4 0.7 mm		FR4 1.3 mm		AlN 0.63 mm		AlN 1 mm	
	ac	USV	ac	USV	ac	USV	ac	USV	ac	USV	ac	USV
Avg (kV)	17.19	14.39	20.30	16.93	17.59	15.59	19.35	16.96	19.64	13.30	19.57	16.90
SD (kV)	2.19	2.06	2.35	2.31	2.36	1.99	2.41	1.26	1.64	1.79	1.66	2.31
95 % CI	18.09	15.24	21.27	17.89	18.56	16.41	20.35	17.48	20.55	14.29	20.48	18.18
UB/LB	16.28	13.54	19.33	15.98	16.61	14.77	18.36	16.43	18.73	12.32	18.65	15.62
p-value	2.23E-04		2.43E-05		6.16E-04		6.47E-04		2.82E-07		2.10E-03	

Synthetic ester												
Barriers	PVC 1 mm		PVC 2 mm		FR4 0.7 mm		FR4 1.3 mm		AlN 0.63 mm		AlN 1 mm	
	ac	USV	ac	USV	ac	USV	ac	USV	ac	USV	ac	USV
Avg (kV)	25.86	20.61	25.54	21.74	25.35	19.85	26.17	20.48	21.56	17.44	23.62	20.05
SD (kV)	3.64	1.72	1.90	3.31	2.89	0.93	3.01	1.53	1.48	2.08	3.96	1.89
95 % CI	27.36	21.32	26.33	23.10	26.54	20.23	27.41	21.11	22.38	18.59	25.81	21.10
UB/LB	24.36	19.90	24.76	20.37	24.15	19.46	24.93	19.85	20.74	16.29	21.43	19.01
p-value	1.69E-08		6.83E-06		3.45E-09		3.35E-08		8.12E-08		1.13E-03	

*Avg: Average, SD: Standard Deviation, CI : Confidence interval, UB : Upper bound, LB : Lower bound

TABLE 6. % Decrease in average PDIV under USV for different barriers tested in two dielectric liquid.

Barriers	PVC		FR4		AlN	
Thickness (in mm)	1	2	0.7	1.3	0.63	1
% Decrease (Mineral oil)	16	17	11	12	32	14
% Decrease (Ester)	20	15	22	22	19	15

**Note: result rounded to nearest integer value*

As demonstrated before (and tested, yet again, by removing needle and power supply to the PMT), these patterns correspond to actual PD events and not to EMI issues. Only a small peak at around 0.4 pC during the rising edge of V_{DC} can be associated with EMI perturbations.

As a conclusion, in addition to the different PDIV values shown in Figs 12 and 13, the optically-acquired PRPD patterns clearly shows a different PD distribution in USV as compared to ac.

VII. CONCLUSION AND PERSPECTIVES

The developed test system is able to generate square waveform with a rise time of about 256 ns across the chosen DUT, leading to a dV/dt of more than 50 kV/μs at 20 kV. A PMT is used for the measurement of PDs to achieve high immunity against the EMIs generated under fast repetitive square voltages. Despite the intrinsic immunity of the optical detection method, associated with some standard EMI mitigation principles, interferences can be observed on the PMT signals during the rising edge of the USV waveform. With the PMT coupled to the oscilloscope, the PD detection is only possible roughly 400 ns after the rise time of USV waveform. Using a dedicated PD measurement system, on the other hand, the noise peak during USV transients is found to be quite close to the background noise level, thanks to its frequency-domain integration. This allows detection of PDs at any instant, with only a moderate increase in the detection threshold.

The synchronized acquisition of PDs with electrical and optical method in ac allow some quantification of the optically-acquired PD values: 0.5 pa.u. from optical detection roughly corresponds to 2 pC in mineral oil and 10 pC of apparent charge in the ester.

The lower average PDIV found under USV waveform shows the initiation of PD activity at a lower voltage under USV than in ac for the used DUT, which has a highly-divergent field. Multiple tests performed with different combinations of solid/liquid reinforce this observation. The PRPD patterns show a different PD distribution in ac and USV; this points to a distinct PD mechanism in USV. This difference could be due to the high dV/dt.

The investigation presented in this paper has demonstrated the capability of the PMT in PD detection under high dV/dt. Improvements are required to overcome the EMIs impacting the transmitted PMT signals, while the PMT detector in itself is insensitive to EMI.

The test system thus developed will provide a platform for further PD investigation by varying DUT parameters (gap, electrodes, transparent media) as well as USV parameters (rise time and switching frequency) to understand their impact on the PD mechanism. Also, this test bench can be exploited for the development of non-conventional PD detection tools under high dV/dt which will be required for non-transparent medium such as solid insulation systems.

APPENDIX

STATISTICAL ANALYSIS USING T-TEST

Usual approach to perform the statistical analysis on datasets available from PD tests is the calculation of average ($\bar{x}$) and standard deviation (SD) values. The average calculates the arithmetic mean of all the observations in a dataset while the SD indicates the spread from the average value. When the average values from two distinct experimental datasets (such as from two different dielectric liquids) differ only slightly, it is essential to determine if the difference is meaningful or merely coincidental. Although, the SD provides the measure of variability between two datasets. But it is not enough to make a firm conclusion when there is a partial overlap in SD bars from two datasets.

To address this, the t-test has been used in this paper to ensure if the difference between average values from two datasets is statistically significant [34]. With two datasets, the t-test is carried out in the following steps:

a. In the first step the null hypothesis is considered which signifies that there is no difference between the average of two datasets.
b. Then, the t-score is calculated for the two datasets in the following way:
   If datasets are from two independent samples, two sample t-test is used to calculate the t-score 't' :

$$t = \frac{(\bar{x}_1 - \bar{x}_2)}{\sqrt{(\frac{s_1^2}{n_1} + \frac{s_2^2}{n_2})}} \tag{A.1}$$

   where, $\bar{x}_1$ = mean of first sample; $\bar{x}_2$ = mean of second sample; s_1 = standard deviation of first sample; s_2 = standard deviation of second sample; n_1 = size of first sample; n_2 = size of second sample
   If variance of two independent samples is equivalent, then $s_1 = s_2$ in (1).
   When two separate datasets from same sample are available, paired sample t-test is performed, which is defined as:

$$t = \frac{\bar{x} - \Delta}{s/\sqrt{n}} \tag{A.2}$$

   where, $\bar{x}$ = mean of sample of differences; Δ = mean difference postulated in null hypothesis; s = standard deviation of sample of differences; n = size of sample of differences
c. The measure of probability of the difference in the average from two datasets, is commonly done by assuming a p-value of 5 %. The p-value is proof that the null hypothesis is false.
d. Finally, a t-distribution look up table is used to estimate the p-value, which corresponds to a p-value for known degree of freedom.
   - If p-value < 0.05 : the null hypothesis is rejected, indicating that there is a significant difference between the average values of two datasets.
   - If p-value > 0.05 : the null hypothesis cannot be rejected, and it means that average of two groups is almost identical.

For ease, the p-value is calculated using T.TEST() function in Microsoft Excel with the experimentally obtained data. The T.TEST() function requires four parameters, array 1, array 2, type of tail distribution and type of sample (paired or two samples). The array 1 and array 2 are the two datasets being compared. Two tailed distributions have been chosen as it is considered appropriate for attaining significance using t-test method. The paired sample is considered if the datasets are from same specimen (e.g., same dielectric liquid in USV and ac), whereas two sample is used when datasets are from two independent specimens (e.g., different dielectric liquids or different barriers).

REFERENCES

[1] C. Gao, W. Wang, S. Song, S. Wang, L. Yu, and Y. Wang, "Localization of partial discharge in transformer oil using Fabry–Pérot optical fiber sensor array," *IEEE Trans. Dielectr. Electr. Insul.*, vol. 25, no. 6, pp. 2279–2286, Dec. 2018, doi: 10.1109/TDEI.2018.007065.

[2] T. Guillod, R. Faerber, D. Rothmund, F. Krismer, C. M. Franck, and J. W. Kolar, "Dielectric losses in dry-type insulation of medium-voltage power electronic converters," *IEEE J. Emerg. Sel. Topics Power Electron.*, vol. 8, no. 3, pp. 2716–2732, Sep. 2020, doi: 10.1109/JESTPE.2019.2914997.

[3] M. Ghassemi, "Accelerated insulation aging due to fast, repetitive voltages: A review identifying challenges and future research needs," *IEEE Trans. Dielectr. Electr. Insul.*, vol. 26, no. 5, pp. 1558–1568, Oct. 2019, doi: 10.1109/TDEI.2019.008176.

[4] M. Jaritz and J. Biela, "Isolation design of a 14.4 kV, 100 kHz transformer with a high isolation voltage (115 kV)," in *Proc. IEEE Int. Power Modulator High Voltage Conf. (IPMHVC)*, San Francisco, CA, USA, Jul. 2016, pp. 73–78, doi: 10.1109/IPMHVC.2016.8012831.

[5] S. Isler, T. Chaudhuri, D. Aguglia, and X. A. Bonnin, "Development of a 100 kW, 12.5 kV, 22 kHz and 30 kV insulated medium frequency transformer for compact and reliable medium voltage power conversion," in *Proc. 19th Eur. Conf. Power Electron. Appl. (EPE ECCE Europe)*, Sep. 2017, p. 10, doi: 10.23919/EPE17ECCEEurope.2017.8099196.

[6] R. Moller, B. Soppe, and A. Schnettler, "Development of a test bench to investigate the breakdown voltage of insulation oil in a frequency range between 1 kHz and 10 kHz," in *Proc. IEEE 2nd Int. Conf. DC Microgrids (ICDCM)*, Jun. 2017, pp. 160–165, doi: 10.1109/ICDCM.2017.8001038.

[7] *High-Voltage Test Techniques—Partial Discharge Measurements: Techniques des Essais á Haute Tension—Mesures des décharges Partielles*, Standard IEC 60270, Internationale Elektrotechnische Kommission, Geneva, Switzerland, 2015.

[8] T. J. A. Hammarstrom, "Partial discharge characteristics at ultra-short voltage risetimes," *IEEE Trans. Dielectr. Electr. Insul.*, vol. 25, no. 6, pp. 2241–2249, Dec. 2018, doi: 10.1109/TDEI.2018.007445.

[9] E. Lindell, T. Bengtsson, J. Blennow, and S. M. Gubanski, "Measurement of partial discharges at rapidly changing voltages," *IEEE Trans. Dielectr. Electr. Insul.*, vol. 15, no. 3, pp. 823–831, Jun. 2008, doi: 10.1109/TDEI.2008.4543120.

[10] *Electrical Insulating Materials and Systems–Electrical Measurement of Partial Discharges (PD) Under Short Rise Time and Repetitive Voltage Impulses*, document IEC 61934, International Electrotechnical Commission, Geneva, Switzerland, 2011.

[11] C. Zhang, M. Dong, B. Wang, and M. Ren, "Partial discharge detection and assessment of surface defects under fast rising repetitive square voltage for MV converter application," in *Proc. IEEE Conf. Electr. Insul. Dielectric Phenomena (CEIDP)*, Richland, WA, USA, Oct. 2019, pp. 311–314, doi: 10.1109/CEIDP47102.2019.9009626.

[12] J. Wu, A. R. Mor, P. V. M. van Nes, and J. J. Smit, "Measuring method for partial discharges in a high voltage cable system subjected to impulse and superimposed voltage under laboratory conditions," *Int. J. Electr. Power Energy Syst.*, vol. 115, Feb. 2020, Art. no. 105489, doi: 10.1016/j.ijepes.2019.105489.

[13] P. Wang, A. Cavallini, G. C. Montanari, and G. Wu, "Effect of rise time on PD pulse features under repetitive square wave voltages," *IEEE Trans. Dielectr. Electr. Insul.*, vol. 20, no. 1, pp. 245–254, Feb. 2013, doi: 10.1109/TDEI.2013.6451364.
[14] A. A. Abdelmalik, A. Nysveen, and L. Lundgaard, "Influence of fast rise voltage and pressure on partial discharges in liquid embedded power electronics," *IEEE Trans. Dielectr. Electr. Insul.*, vol. 22, no. 5, pp. 2770–2779, Oct. 2015, doi: 10.1109/TDEI.2015.005411.
[15] L. E. Lundgaard, "Partial discharge. XIV. Acoustic partial discharge detection-practical application," *IEEE Elect. Insul. Mag.*, vol. 8, no. 5, pp. 34–43, Sep. 1992, doi: 10.1109/57.156943.
[16] K. Wu, T. Okamoto, and Y. Suzuoki, "Effects of discharge area and surface conductivity on partial discharge behavior in voids under square voltages," *IEEE Trans. Dielectr. Electr. Insul.*, vol. 14, no. 2, pp. 461–470, Apr. 2007, doi: 10.1109/TDEI.2007.344627.
[17] G. C. Montanari, R. Hebner, P. Seri, and R. Ghosh, "Noise rejection and partial discharge identification in PDIV tests of insulated wires under repetitive impulse supply voltage," in *Proc. IEEE Electr. Insul. Conf. (EIC)*, Calgary, AB, Canada, Jun. 2019, pp. 505–508, doi: 10.1109/EIC43217.2019.9046587.
[18] C. G. A. Ramos, "Partial discharge phenomena in converter and traction transformers—Identification and reliability," Ph.D. Thesis, Univ. Bologna, Bologna, Italy, 2014.
[19] T. Koltunowicz, A. Cavallini, D. Djairam, G. C. Montanari, and J. Smit, "The influence of square voltage waveforms on transformer insulation break down voltage," in *Proc. Annu. Rep. Conf. Electr. Insul. Dielectric Phenomena*, Cancun, Mexico, Oct. 2011, pp. 48–51, doi: 10.1109/CEIDP.2011.6232593.
[20] Z. D. Wang, Q. Liu, X. Wang, X. Yi, P. Jarman, G. Wilson, P. Dyer, F. Perrot, C. Perrier, D. Walker, M. Lashbrook, and J. Noakhes, "Ester insulating liquids for power transformers," CIGRE, Paris, France, Tech. Rep. CIGRE A2-209, 2012.
[21] S. Anand, E. Vagnon, A. Zouaghi, M. Guillet, C. Buttay, and O. Agri, "Electrical and optical partial discharge assessment of dielectric barriers in mineral oil and synthetic ester," in *Proc. IEEE Electr. Insul. Conf. (EIC)*, Denver, CO, USA, Jun. 2021, pp. 602–605, doi: 10.1109/EIC49891.2021.9612267.
[22] Z. Wei, H. You, R. Na, and J. Wang, "Partial discharge detection strategies under fast rise time voltages generated by wide-bandgap semiconductor devices," in *Proc. IEEE Electr. Insul. Conf. (EIC)*, Calgary, AB, Canada, Jun. 2019, pp. 75–78, doi: 10.1109/EIC43217.2019.9046572.
[23] M. Muhr and R. Schwarz, "Experience with optical partial discharge detection," in *Proc. Int. Conf. Adv. Process. Test. Appl. Dielectr. Mater. Wroclaw Pol.*, Poland, 2007, pp. 26–29. [Online]. Available: https://graz.pure.elsevier.com/en/publications/experience-with-optical-partial-discharge-detection
[24] *Photomultiplier Tubes: Basics and Applications*, 3A ed. Japan: Hamamatsu, [Online]. Available: https://www.hamamatsu.com/resources/pdf/etd/PMT_handbook_v3aE.pdf
[25] BEHLKE. *Fast High Voltage Transistor Switches*. [Online]. Available: https://www.behlke.com/pdf/general.pdf
[26] (Apr. 2011). *Good Titration Practices for Karl Fischer Titration*. Mettler Toledo, Switzerland, Brochure. [Online]. Available: https://www.mt.com/dam/non-indexed/po/ana/titration/51725145B_V10.11_GTP_KF_Titr_HB_Complet.pdf
[27] *MIDEL-7131-Product Brochure*. [Online]. Available: https://www.midel.com/app/uploads/2018/05/MIDEL-7131-Product-Brochure.pdf
[28] NYNAS.*Nytro 4000X: Datasheet*. [Online]. Available: https://www.barth-gmbh.at/resources/PDS_Nytro_4000X_EN.pdf?label=RESOURCE_PDS_Nytro_4000X_EN.pdf_EN
[29] V. W. L. Chin, T. L. Tansley, and T. Osotchan, "Electron mobilities in gallium, indium, and aluminum nitrides," *J. Appl. Phys.*, vol. 75, no. 11, pp. 7365–7372, Feb. 1994, doi: 10.1063/1.356650.
[30] M. Florkowski, D. Krześniak, M. Kuniewski, and P. Zydroń, "Partial discharge imaging correlated with phase-resolved patterns in non-uniform electric fields with various dielectric barrier materials," *Energies*, vol. 13, no. 11, p. 2676, May 2020, doi: 10.3390/en13112676.
[31] S. Anand, E. Vagnon, M. Guillet, and C. Buttay, "Assessment of partial discharge phenomenon in AC and fast-rising square voltage using optical detection technique in needle-plane configuration with pressboard in mineral oil," in *Proc. IEEE 21st Int. Conf. Dielectric Liquids (ICDL)*, May 2022, pp. 1–4, doi: 10.1109/ICDL49583.2022.9830959.
[32] X. Yang, Y. Ming, C. Xiaolong, Q. Changrong, and G. Chen, "Comparison between optical and electrical methods for partial discharge measurement," in *Proc. 6th Int. Conf. Properties Appl. Dielectric Mater.*, Xi'an, China, 2000, pp. 300–303, doi: 10.1109/ICPADM.2000.875690.
[33] V.-H. Dang, A. Beroual, E. A. Al-Ammar, and M. Qureshi, "Comparative PD characteristics of pressboard/mineral oil and pressboard/vegetable oil insulating systems," in *Proc. IEEE Int. Conf. Condition Monitor. Diagnosis*, Bali, Indonesia, Sep. 2012, pp. 890–893, doi: 10.1109/CMD.2012.6416294.
[34] P. Dusart. (2018). *Cours de Statistiques Inférentielles*. Université de Limoges. [Online]. Available: https://www.unilim.fr/pages_perso/pierre.dusart/Probas/cours_stat_S4.pdf

SOMYA ANAND received the B.Tech. degree from the University of Uttarakhand, Dehradun, India, in 2011, the master's degree in electrical engineering from Institut Polytechnique de Grenoble, France, in 2018, and the Ph.D. degree from Université de Lyon, France, in 2022. From 2012 to 2016, he was an Electrical Engineer at private sector. Since 2018, he has been with the joint venture between the SuperGrid Institute and the Ampère Laboratory to address the insulation constraints generated by power electronic switches, with a main focus on partial discharge measurements. Currently, he is working on different types of sensors to measure partial discharges under high dV/dt.

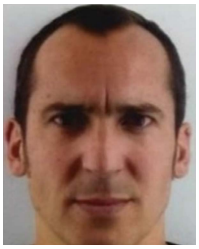

ERIC VAGNON (Member, IEEE) received the French National Teaching degree (Agrégation) in electrical engineering from the Université Claude Bernard Lyon 1, in 2005, and the Ph.D. degree from the University Grenoble Alpes, in 2010. He was a Research Engineer in the field of 3-D packaging for silicon power devices or the development of liquid metal spreaders for power modules. Since 2016, he has been an Associate Professor with the Ecole Centrale de Lyon and the Ampere Laboratory. He is also a part of the SuperGrid Institute, he defines insulation solutions for medium-frequency transformers and in packaging activities. His research interests include high-voltage engineering, dielectric materials characterization, and partial discharge measurement.

MARTIN GUILLET received the M.Sc. degree in general engineering from Ecole Centrale de Lyon, France, in 2006. From 2006 to 2017, he was at Varioptic, Lyon, France on the design of opto-electronic components. Since 2017, he has been involved in the design of medium frequency transformers with the SuperGrid Institute, Lyon, where he has been the Leader of the Medium Frequency Transformers Research Team, since 2019.

CYRIL BUTTAY (Senior Member, IEEE) received the engineering and Ph.D. degrees from the Institut National des Sciences Appliquées (INSA) Lyon, Lyon, France, in 2001 and 2004, respectively.

From 2005 to 2007, he was a Research Associate at the Electrical Machines and Drives Research Team, University of Sheffield, Sheffield, U.K., and the Power Electronics Machines and Control Group, University of Nottingham, Nottingham, U.K. Since 2008, he has been a Scientist with the French Centre National de Recherche Scientifique (CNRS), where he was with the Ampére Laboratory, Lyon, on the topic of packaging for power electronics, with a special focus on high-temperature, high-voltage, or high-density applications. He is currently a Visiting Scholar with the Center for Power Electronics Systems (CPES), Virginia Tech, Blacksburg, VA, USA, and the Deputy Director of Ampére Laboratory.